

MODELLING DISCONTINUOUS-LONG-FIBRE COMPOSITES IN TENSILE SPECIMEN TESTING

Belliveau, R¹, Landry, B^{1*}, and LaPlante, G¹

¹ Département de génie mécanique, Université de Moncton, Moncton, Canada

* Corresponding author (benoit.landry@umoncton.ca)

Keywords: *DLF composites, Finite element modelling*

ABSTRACT

Discontinuous-long-fibre (DLF) composites fabricated by compression moulding pre-impregnated UD fibre chips are generating interest in the aerospace and automotive industries. These composites benefit from the high volume fraction of prepregs while allowing the fabrication of complex shape parts. However, the effects of the random nature of chip distribution compounded by the orthotropic chip properties make the mechanical behaviour of compression moulded DLF composites difficult to predict. Local weaknesses may be present within the material when chips are unfavorably oriented with respect to the load, thereby reducing the mechanical properties and increasing their variability. To better understand the behaviour of these composites, a finite element model was developed to predict the mechanical properties obtained from a tensile test. DLF chips were modelled based on a voxel method where random chip positions were generated by an algorithm developed in this work. ANSYS® software was used to model the non-linear phenomena and damage response of the composite. The Puck failure criteria was used to model damage initiation in the specimen. Tensile modulus and strength predictions showed good correlation with experimental results. It appeared that the failure of the UD fibre DLF composite was associated with matrix failure (transverse tension and in-plane shear).

1 INTRODUCTION

Compression moulded discontinuous-long-fibre composites (DLF) research has recently generated a lot of interest in specialized industries such as aerospace and automotive. DLF composites show a great potential for recycling continuous fibre off-cuts and remnants from manufacturing by remoulding the scraps [1, 2]. The DLF composites architecture take advantage of the high volume fraction (v_f) of the pre-impregnated continuous fibres, which ranges from 50-60%, while maintaining the ability to form complex shapes [3], thus helping to bridge the gap between continuous-fibre and short-fibre composites [4]. DLF composites start as a continuous-fibre prepreg tape, which is cut and slit into chips. These chips are then compression moulded into the required geometry. Studies show that DLF composites may have stiffnesses comparable to those of continuous-fibre quasi-isotropic laminates, but their strength is significantly lower [3, 5].

Early studies suggested that in-plane isotropy can be achieved in DLF composites [3]. However, recent studies have shown that when chip flow is encountered during moulding, in-plane isotropic properties can no longer be assumed [6–9]. Chip flow leads to fibre alignment in the direction of flow, creating a highly anisotropic material where lower properties are encountered perpendicular to the flow. Furthermore, using digital imaging correlation, some researchers have observed highly nonuniform strain fields caused by variability in fibre orientation [5, 10]. Weak points in the material due to unpreferred chip

orientations is a source of serious concern in load bearing components, as well as the high variability in mechanical properties shown by Feraboli *et al.* [6].

To better understand the underlying phenomena governing the mechanical behaviour of DLF composites, a finite element model (FEM) was developed in this study. A model proposed by Selezneva [11], where 2D solid elements were employed for simplification, showed promising results. To consider the randomness of the DLF composite, partitions in the specimen were created to assign random stack up orientations and sequences. These stack ups were defined by a position algorithm, from which the ABD matrix of the classic laminate theory could be calculated. Hashin's failure criteria was used to model the initiation of progressive damage in the composite. That study was limited to the 2D response of the elements. The present study proposes using 3D elements to better represent the specimen behaviour. An algorithm developed to generate the random 3D positioning of the DLF chips is described in this work. This algorithm is utilized to generate a FEM that predicts the results of standard tensile tests with DLF specimens. Model validation was performed by comparing the FEM results to experimental results from a previous study [12].

2 DISCRETIZATION OF THE COMPUTING DOMAIN

The discretization of the geometry was carried out with a method similar to the one used by Selezneva *et al.* [11]. However, the model developed here is composed of a 3D solid brick elements, which makes it possible to evaluate the effect of the stacking sequence of the pre-impregnated fibre chips. The principle of the method is to assign an in-plane orientation to each of the elements in the model to represent the chips. To do this, an algorithm was developed to position the chips randomly within the domain. Since the algorithm is based on the element numbers, it is important that the geometry be previously discretized with a structured mesh.

For this model, ANSYS [13] SOLID185 eight-node elements were chosen. The elements must be significantly smaller than the chips for good accuracy, as shown by Selezneva [11]. The size of the elements selected for this work is $0.5 \text{ mm} \times 0.5 \text{ mm} \times t$ (where t is the thickness of the chips), which constituted a good compromise between the accuracy of the model and the calculation time. The procedure can be viewed as one in which chips are placed arbitrarily one-by-one in the mould until it is completely filled. This is accomplished by successively assigning in-plane orientations to a group of elements representing a chip, until all elements have been processed. Each chip is first given a completely random orientation (θ) and position (X, Y) in the XY plane as shown in Figure 1. The constructed model represents a tensile specimen for which the X position varies from 0 to L , the Y position varies between 0 and H and the chip orientation angle varies between -90° and 90° . Uniform statistical distributions were used for the position and orientation of the chips. The lengths (L) and width (H) were defined as 150 mm and 25 mm, respectively, to represent the experimental tests from a previous study [12]. Chips dimensions were set as $12.7 \text{ mm} \times 12.7 \text{ mm}$ as in the experimental tests.

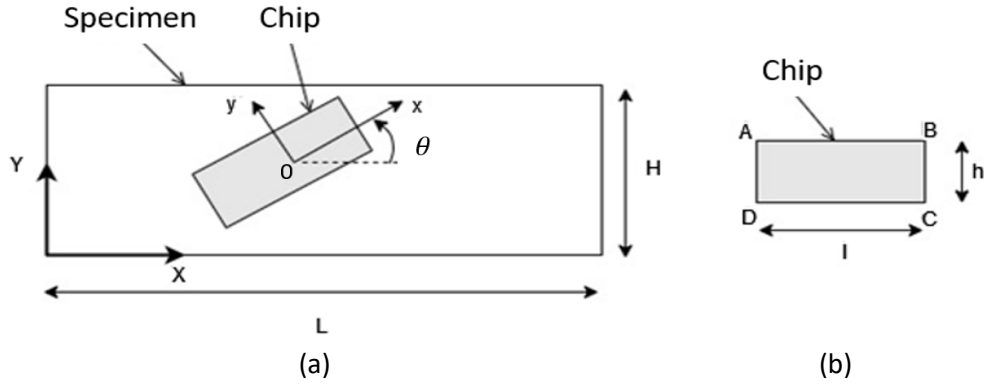


Figure 1 – (a) Random positioning of the chips. (b) Chips size.

Elements in the area covered by a chip meet the criterion

$$ABe + ADe + DCe + BCe \leq l \cdot h \quad (2)$$

where

$$ABe = \left| \frac{(X_A \cdot Y_B) + (X_B \cdot Y_e) + (X_e \cdot Y_A) - (Y_A \cdot X_B) - (Y_B \cdot X_e) - (Y_e \cdot X_A)}{2} \right|$$

$$ADe = \left| \frac{(X_A \cdot Y_C) + (X_C \cdot Y_e) + (X_e \cdot Y_A) - (Y_A \cdot X_C) - (Y_C \cdot X_e) - (Y_e \cdot X_A)}{2} \right|$$

$$DCe = \left| \frac{(X_C \cdot Y_D) + (X_D \cdot Y_e) + (X_e \cdot Y_C) - (Y_C \cdot X_D) - (Y_D \cdot X_e) - (Y_e \cdot X_C)}{2} \right|$$

$$BCe = \left| \frac{(X_D \cdot Y_B) + (X \cdot Y_e) + (X_e \cdot Y_D) - (Y_D \cdot X_B) - (Y_B \cdot X_e) - (Y_e \cdot X_D)}{2} \right|$$

represent the areas of the triangles formed by connecting the corners of the chip to the centroid of the evaluated element (x_e, y_e) . A given element is included if the sum of these areas is less than or equal to the area of the chip.

The first chip to be placed will always occupy space associated with elements from the first layer. Thereafter, when a chip (or part of a chip) is placed in an occupied space, there will be superposition. To determine the Z position occupied by an element of chip, a Z -position indicator matrix is defined. This matrix is first initialized to zero, indicating that the first chip belongs to the initial layer of elements. Each time a chip is placed, all elements in the area covered by that chip have their Z -position indicator increased by 1. With a structured mesh, this scheme can easily link a given chip to element numbers in the model. The number of each element representing a chip is given by

$$E_{num} = E_{XY} + I_{z-pos} \cdot Q_{XY} \quad (3)$$

where E_{XY} is the element number of the first layer, I_{z-pos} is the Z -position indicator of the element of interest, and Q_{XY} is the total number of elements in the XY plane. Figure 2 shows a simple example of a model having 16 elements in which three chips are being randomly positioned. For simplicity, chip orientation is omitted in the figure. Figure displays the evolution of the Z -position indicator matrix and how the element numbers are identified when there are chips stacked on top of each other. Initially the matrix of Z -position indicators consists of only zeros. Then, a chip is positioned and the numbers of the elements (p_{b1}) are defined according to equation (3). Subsequently, the Z -position indicator matrix is updated. The second chip is then randomly placed and its element numbers (p_{b2}) are found based on the newly updated Z -position indicator matrix. The process continues until the volume is completely filled.

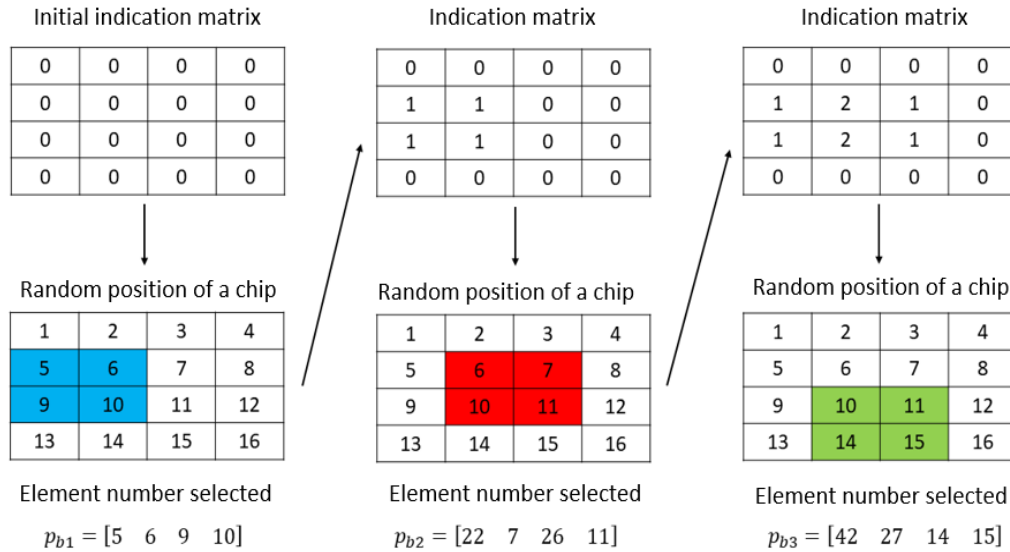


Figure 2 – Example of a simple model having 16 elements, where three chips are positioned randomly.

Once an element is linked with a chip, the randomly allocated chip angle θ is assigned to this element by defining local coordinate system based on the angle of the chip. An example of a discretized model is shown in Figure 3. The thickness of the elements must be equal to the thickness of the chips. However, the length and width of the chips need to be specified. This makes it possible to model virtually any size of chips while keeping good accuracy, as long as the element size is significantly smaller than the chip size.

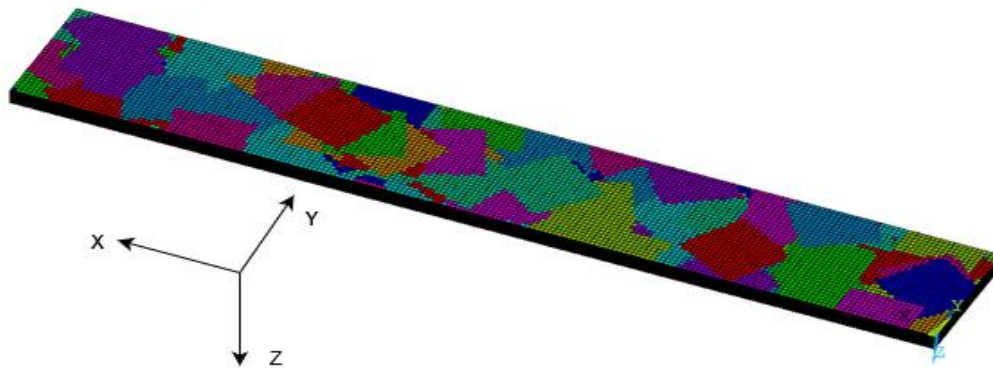


Figure 3 – Example of a discretized model. Colours represent the coordinate systems assigned to the elements.

3 MODEL DEFINITION

3.1 Mechanical behaviour

The mechanical properties of the composite from which the chips are derived are presented in Table 1. Properties that are not asterisked are taken from the material supplier’s data [14].

Table 1 – Mechanical properties of the composite chips used for numerical analysis [14].

Property	Value	Property	Value
E_{11} [GPa]	120*	X_t [MPa]	2241
$E_{22}(E_{33})$ [GPa]	9*	X_c [MPa]	1200
$G_{12}(G_{13})$ [GPa]	5.2	Y_t [MPa]	92
G_{23} [GPa]	4	Y_c [MPa]	92
$\nu_{12}(\nu_{13})$	0.29	S_{12} [MPa]	141
ν_{23}	0.4		

* Property measured by the authors

To model the non-linear behaviour of the composite, a progressive damage model was used. This model reduces the rigidity of the elements that have suffered a failure. The modified Puck’s failure criterion was chosen [13] to govern damage initiation. Three damage variables reduce the rigidity of the elements: damage in direction 1 (d_1), damage in direction 2 (d_2) and in-plane shear damage (d_{12}). The stress-strain relationship is given by

$$\sigma = [D]\varepsilon \quad (4)$$

where the elasticity matrix is

$$[D] = \begin{bmatrix} \frac{C_{11}}{(1-d_1)} & C_{12} & C_{13} & 0 & 0 & 0 \\ C_{21} & \frac{C_{22}}{(1-d_2)} & C_{23} & 0 & 0 & 0 \\ C_{31} & C_{32} & \frac{C_{33}}{(1-d_2)} & 0 & 0 & 0 \\ 0 & 0 & 0 & \frac{C_{44}}{(1-d_{12})} & 0 & 0 \\ 0 & 0 & 0 & 0 & \frac{C_{55}}{(1-d_{12})} & 0 \\ 0 & 0 & 0 & 0 & 0 & \frac{C_{66}}{(1-d_{12})} \end{bmatrix}^{-1}$$

3.2 Puck’s model

To determine whether the material suffers damage, the modified Puck failure criterion [13] was used. According to this model, the failure criterion in direction 1 (i.e., direction parallel to the fibres) is defined by

$$f_1 = \left| \frac{\sigma_1}{X} \right| \quad (5)$$

where

$$X = \begin{cases} X_c, & \sigma_1 < 0 \\ X_t, & \sigma_1 \geq 0 \end{cases}$$

The failure criterion in direction 2 (i.e., failure of the matrix) is defined by

$$f_2 = \frac{\sigma_2^2}{Y_t Y_c} + \frac{\tau_{12}^2}{S^2} + \left(\frac{1}{Y_t} + \frac{1}{Y_c} \right) \sigma_2 \quad (6)$$

where σ_1 , σ_2 and τ_{12} represent the stress in direction 1, the stress in direction 2 and the shear stress in plane 12, respectively. Puck's model is therefore defined as

$$f = \max(f_1, f_2)$$

where the element fails when f is greater than 1.

3.3 Damage variables

Damage variables are used to reduce the stiffness of the material at the locations where failure occurs. This reduction in stiffness allows the modelling of progressive damage, i.e., the evolution of damage in the elements. Damage variables behave as follows:

$$d_1 = \begin{cases} 0, & f_1 < 1 \\ 0.95, & f_1 \geq 1 \end{cases} \quad d_2 = \begin{cases} 0, & f_2 < 1 \\ 0.95, & f_2 \geq 1 \end{cases} \quad d_{12} = \begin{cases} 0, & f_2 < 1 \\ 0.95, & f_2 \geq 1 \end{cases} \quad (7)$$

The damage variables vary between 0 and 0.95, where 0 represents no damage and 0.95 represents the maximum damage to the element.

3.4 Conditions of the analysis

Due to the random behaviour of the model, ten specimens were tested by simulation. This makes it possible to perform statistical analyses, as well as to validate the model by comparing it with the experimental results obtained previously [12]. The boundary conditions shown in Figure 4 were used to represent the conditions of the tensile tests. Uniform displacement in positive X -direction is applied to the nodes at the right end, while the nodes at the left end are fixed in the X -direction. To fix the model in the Y and Z directions, a node at each end of the model blocks the movement in those directions. These are represented by the red dots in Figure 4. These boundary conditions are imposed to represent a sample fixed in the jaws of a tensile testing apparatus.

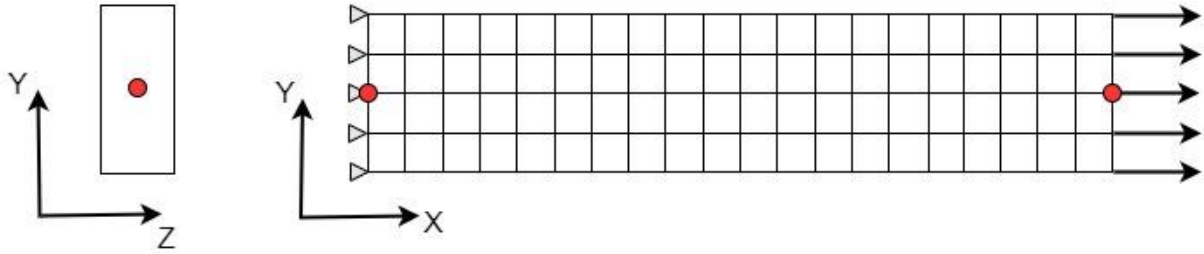


Figure 4 – Boundary conditions of the finite element analysis model.

4 RESULTS

A summary of the results obtained is shown in Figure 5, where the bars represent the average, the error bars represent the standard deviation, and the square dots represent the extreme values. Tensile strengths and tensile moduli are compared in these graphs. The data include ten simulations.

An analysis of variance (ANOVA) is used to validate the data, with an alpha limit of 5%. The ANOVA analysis compares numerical results with experimental values. The P-values of these analyses are presented in Table 2.

These results show that the model can accurately predict the modulus of DLF composites, including the variability. In addition, the model adequately represents the average strength, but its predicted strength variability is smaller than the experimental variability. Figure 6 shows failure modes present within the specimen.

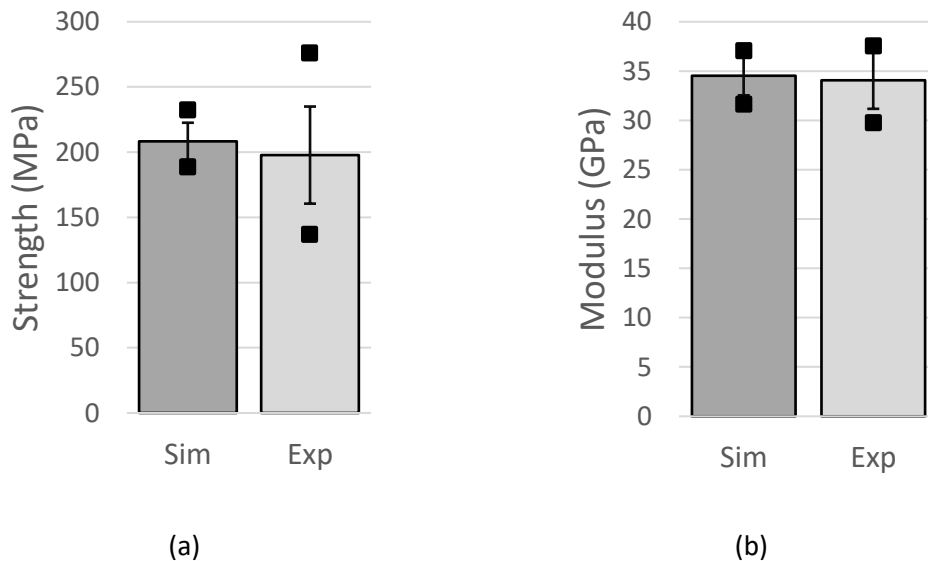


Figure 5 – Comparison of the mechanical properties for simulation (Sim) and experimental (Exp) data. (a) Tensile strength and (b) Tensile modulus.

Table 2 – P-values obtained for the comparison between numerical and experimental analyses.

	P-value
Strength UD fibres	< 0.05
Modulus UD fibres	0.61

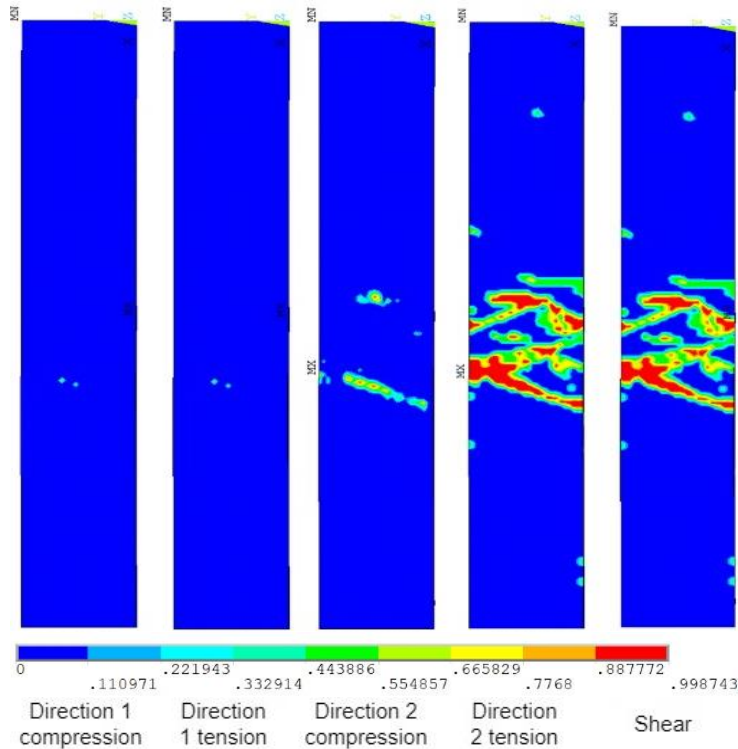


Figure 6 – Failure modes predictions for the DLF composite. The scale represents the damage, where 0 means no damage and 1 means the complete rupture of the element.

5 DISCUSSION

The results of this numerical analysis show that the proposed method shows great potential to predict the average properties of DLF composites. The average and the variability in the modulus showed a good correlation with the experimental results. The lower variability in the simulation results for the strength is suspected to be caused by the perfectly uniform distribution of chip orientation used in the model. Although, uniform distribution is assumed to represent the fabrication process, some preferential angle tendencies are bound to happen in practice, which may influence the results. This needs to be further studied. Figure 6 reveals that the failure of specimens with UD chips is mainly caused by the rupture in direction 2 of the material, i.e., the direction perpendicular to the fibres. Shear failure is also very apparent. These failure modes are associated with matrix failure. Fibre breakage is practically non-existent. Unpreferred chip orientation cause weaknesses in the material and failure occurs at those locations. It is hypothesised that using woven fibre chip in DLF could alleviate this problem and yield mechanical improved properties. Work is currently underway to verify this hypothesis.

6 CONCLUSION

In sum, this study presented a simple but efficient way to simulate the mechanical behaviour of DLF composites made from pre-impregnated chips. The proposed FEM, based on 3D solid elements, was fully developed using ANSYS software without requiring external software to discretize the domain. By using progressive damage features, the model can predict the strength and modulus of DLF specimens.

The proposed model was used to better understand the mechanical behaviour of DLF composites fabricated from UD chips. Simulation and experimental data showed good correlation, thus suggesting great potential for the modeling technique. From this analysis, it was concluded that the in-plane orthotropic properties of the UD chips have a large impact on the failure mechanism of the material.

7 REFERENCES

- [1] Pickering SJ. Recycling technologies for thermoset composite materials - current status. *Compos Part A* 2006; 37: 1206–1215.
- [2] Leblanc D, Landry B, Jancik M, *et al.* Recyclability of Randomly-Oriented Strand Thermoplastic Composites. 20th International Conference on Composite Materials, Copenhagen, July 2015.
- [3] Feraboli P, Peitso E, Deleo F, *et al.* Characterization of Prepreg-Based Discontinuous Carbon Fiber/Epoxy Systems. *J Reinf Plast Compos* 2009; 28: 1191–1214.
- [4] Eguémann N. Processing of characterisation of carbon fibre reinforced PEEK with discontinuous architecture. 16th European Conference on Composite Materials ECCM16, Seville, June 2014.
- [5] Feraboli P, Peitso E, Cleveland T, *et al.* Modulus Measurement for Prepreg-based Discontinuous Carbon Fiber/Epoxy Systems. *J Compos Mater* 2009; 43: 1947–1965.
- [6] Feraboli P, Cleveland T, Ciccu M, *et al.* Defect and damage analysis of advanced discontinuous carbon/epoxy composite materials. *Compos Part A Appl Sci Manuf* 2010; 41: 888–901.
- [7] Belliveau R, Léger É, Landry B, *et al.* Measuring fibre orientation and predicting elastic properties of discontinuous long fibre thermoplastic composites. *J Compos Mater* 2020; 55: 10.
- [8] Léger É, Landry B, LaPlante G. High flow compression molding for recycling discontinuous long fiber thermoplastic composites. *J Compos Mater* 2020; 54: 3343–3350.
- [9] Sommer DE, Kravchenko SG, Denos BR, *et al.* Integrative analysis for prediction of process-induced, orientation-dependent tensile properties in a stochastic prepreg platelet molded composite. *Compos Part A Appl Sci Manuf* 2020; 130: 105759.
- [10] Selezneva M, Lessard L. Characterization of mechanical properties of randomly oriented strand thermoplastic composites. *J Compos Mater* 2016; 50: 2833–2851.
- [11] Selezneva M. Experimental and Theoretical Investigations of Mechanical Properties of Randomly-Oriented Strand (ROS) Composites, Doctoral Thesis, McGill University, Montreal, 2015.
- [12] Belliveau R, Landry B, LaPlante G. Comparative Study of the Mechanical Properties of Woven and Unidirectional Fibres in Discontinuous Long-Fibre Composites, *J Therm Compo Mater* 2022.
- [13] Ansys Help [Online]. Available : ansyshelp.ansys.com (accessed Sep. 08, 2021).
- [14] Toray Cetex® TC1000 Product Data Sheet, Toray Advanced Composites, 2019.